Electronic supplementary material

Loscher et al.: Timing of head movements is consistent with energy minimization in walking ungulates

List of electronic supplementary materials

1. Processing of motion capture data (below)
2. Approximation of the instantaneous position of the head-neck COM (below)
3. Detailed description of the model (below)
4. Video of motion capture data during walking of the reference individual (warmblood gelding Leroy)
5. MATLAB source code and raw data that was used to calculate model parameters, including marker displacement amplitudes and phase relationships of the reference individual
6. MAPLE worksheet for the model

1. Processing of motion capture data

Five utilizable sets of data were recorded for the reference individual (warmblood gelding Leroy) that each allowed all markers to be obtained for at least one full stride. Motion capturing of warmblood horses was part of a larger study that involved a total number of 22 landmarks. Not all markers were used for the purposes of the current paper. The aforementioned software APAS was used to digitize absolute marker positions. To reduce signal noise the recorded data were filtered using the described low-pass filter. All further processing of data relied upon numerical calculations executed in MATLAB (Release 2013b, The MathWorks, Inc., Natick, MA, USA). The corresponding source code is available as part of the electronic supplementary materials.

First, for each set of data, the instants of time when a full stride began and ended were determined. The beginning of the stride was marked manually, for which the instant when the forelimb facing the camera established ground contact was decisive. Subsequently, the instant when the stride ended was automatically identified by selecting the time frame in which the square norm of the vertical deviation of all markers relative their positions in first time frame was at its minimum.

Second, a rotational transformation was applied to all markers. This was necessary, because the direction of locomotion of the individual deviated from the horizontal axis of the recording equipment's reference coordinate system by a small angle. This was done for all markers individually by evaluating trigonometric relations considering absolute distances between marker positions at the beginning and end of a stride, respectively.

Third, a translational transformation was applied to all markers to migrate from the stationary coordinate systems to the relative one that is carried with the reference individual at mean speed of locomotion. In addition, the mean velocity v_m was calculated by averaging the derived horizontal speeds of all markers for all sets of data.

Fourth, all sets of data were rescaled to the same number of 100 time frames. Due to slight deviations in duration of a full stride, every set of data had originally lasted a different number of total frames. Coordinates of marker positions were transferred using linear interpolation, and the duration of all six sets of data was set to the average duration of a stride. This standardization of the resolution of time allowed for the final averaging of the different sets of data into one single reference set.

Finally, data for the far side of the reference individual, which was not facing the camera and thus could not be filmed, were added. Since the movements of contralateral extremities match each other with a phase shift of 50% of the duration of a full stride, marker positions were simply taken over from the corresponding time frames. Furthermore, data for markers of both sides of the sagittal plane were averaged to derive the penetration point of the axis running through the same markers on both sides with the sagittal plane.

A video of the reference set of markers over a complete stride is included in the electronic supplementary materials. In the animation, markers on the right hand side of the sagittal plane are shown in blue, those on the left hand side in red, and those located in sagittal plane in green.

2. Approximation of the instantaneous position of the head-neck COM

Based on published data of Buchner et al.[1] for head and neck segment masses, the position of the segments' COMs, and our own motion capture data, we approximated the instantaneous position of the head-neck unit's COM in the reference individual. For this, both the neck and the head were considered rigid bodies. First, we linearly scaled the published positions of the segment COMs to the size of our reference individual (warmblood gelding Leroy). Next, we determined the segment COM positions relative to the known motion capturing marker positions using the anatomical drawing of Buchner et al. and accepted the introduction of slight inaccuracy resulting from this approach. By this, we migrated the segments COM positions into our motion capture reference system. Motion capture data provided marker positions over time. Subsequently, we used trigonometric relations to determine the instantaneous segments COM location over time relative to the motion capture data. Finally, we determined the location of the combined head-neck unit's COM by mass-weighted superposition of its individual parts. This method accounts for the relative motion between head and neck, their different masses and the resulting influence on the head-neck unit's COM position.

3. Detailed description of the model

In this study, the influence of the observed head nodding behaviour on the primary energy cost of locomotion, namely the amount of work to be performed by the limbs, was analysed. The energetics of head nodding itself, which is performed primarily passively utilizing dynamic energy exchange mechanisms, have been discussed elsewhere[2,3,4].

All analyses described above were subsequently carried out analytically utilizing the computer algebra system Maple (version 12.0, Maplesoft, Waterloo, ON, Canada). The corresponding worksheet is available as part of the electronic supplementary materials.

In the model, the SP displayed a vertical oscillatory movement which, in the horse, is resulting not only from inverse pendulum kinematics[5], but also from the shortening and extension of the supporting legs during double support. The mechanical work thus performed was calculated to determine the model's relative energy expenditure with respect to the phase shift between the vertical oscillatory movements of head-neck unit and the suspension point (SP). At any given moment, the force necessary at the SP to support the head-neck unit in vertical direction (F_y; Fig. ESM1) is determined by:

$$F_y(t,\vartheta) = m_{hn}(g + \frac{d^2}{dt^2} y_{hn}(t,\vartheta))$$

Here, $y_{hn}(t,\vartheta)$ is the vertical coordinate of the COM of the head-neck unit. Furthermore, g is gravitational acceleration and ϑ is the phase shift between the head-neck unit and the SP, which was defined as the angular ratio of time difference between instants when the COM of the head-neck unit (t_{hn}) and the SP (t_{sp}) reach their respective maximum positions in vertical direction:

$$\vartheta = 4\pi \frac{t_{sp} - t_{hn}}{\Delta t_S}$$

Motion capture analysis of the reference individual yielded an average amplitude of this coordinate of $A_{hn} = 3.84\ cm$ relative to its mean height of $h_{hn} = 1.40\ m$ during the phase of limb support. The input kinematics to the model are shown in Fig. ESM2. A discrete Fourier transformation (DFT) of the coordinate's progression showed that all higher-frequency parts of it were at least one order of magnitude lower than that of the predominant fundamental oscillation. They were, therefore, not considered in the further analysis. Thus, a sinusoidal oscillation with an angular frequency of

$\omega = 4\pi f_S$, with $f_S = \frac{1}{\Delta t_S}$ being the stride frequency, could be used to adequately approximate the observed kinematics of the COM:

$$y_{hn}(t, \vartheta) = A_{hn} \sin(\omega t + \vartheta) + h_{hn}$$

To achieve redirection of impulse with minimal effort, ground reaction forces were modelled here to be acting exclusively along the supporting limbs (but see experimental data that documented deviations from this assumption[6]). Consequently, no moments were permitted to act on the SP as a result of limb activity. To determine the forces exerted in the direction of the forelimbs, we discriminated between single limb support (ss) and double limb support (ds). The horizontal component of the force exerted towards the limb in single support was:

$$F_x^{ss}(t, \vartheta) = \frac{l_x(t)}{l_y(t)} F_y(t, \vartheta)$$

Here, lengths l_x and l_y describe the instantaneous horizontal and vertical distances between SP and location of limb ground contact (Fig. ESM1). The power of the limb was hence calculated as:

$$P^{ss}(t, \vartheta) = F_x(t, \vartheta)(v_m + \Delta v_{hsp}(t)) + F_y(t, \vartheta) v_{sp}(t)$$

Here, $v_m + \Delta v_{hsp}(t)$ and $v_{sp}(t)$ are the velocities of the SP in horizontal and vertical directions, respectively. The constant v_m represents the mean velocity of locomotion and was defined by the product of step length l_S and step frequency f_S. The observed deviation from constant velocity was accounted for by $\Delta v_{hsp}(t)$, while $v_{sp}(t)$ stands for the absolute velocity of the SP in vertical direction. Their values were calculated using the relations:

$$v_m = l_S f_S \qquad v_{sp} = \frac{d}{dt} y_{sp}(t) \qquad \Delta v_{hsp} = \frac{d}{dt} \Delta x_{sp}(t)$$

For the vertical coordinate of the SP, motion capture data could be approximated with adequate precision using a simple sinusoidal oscillation. As with the vertical motion of the head-neck unit's COM, negligibility of higher frequencies was shown by evaluation of the DFT of the respective motion capture

data. During the phase of limb support, for the SP's vertical oscillation an amplitude of A_{sp} = 2.97cm at a mean height of h_{sp} = 1.51m was measured:

$$y_{sp}(t) = A_{sp}\sin(\omega t) + h_{sp}$$

Deviations of the horizontal coordinate $\Delta x_{sp}(t)$ of the SP relative to the reference individual's coordinate system did not display such obvious harmonic oscillatory characteristics. To allow for analytic treatment, the coordinate's progression was therefore approximated by a spline interpolation of third degree, which also ensured sufficient continuous differentiability.

We then integrated the calculated power for the duration of single support over time to derive positive and negative mechanical work. Single support began at t_B(ss) and ended at t_E(ss):

$$W^{ss+/ss-}(\vartheta) = \frac{1}{2}\int_{t_B(ss)}^{t_E(ss)} (P^{ss}(t,\vartheta) \pm \left|P^{ss}(t,\vartheta)\right|)\, dt$$

Accordingly, from the beginning t_B(ds) to the end t_E(ds) of double support (ds), the forces directed towards the leading limb (ll; the leading limb has contact first) and the trailing limb (tl), respectively, were determined as follows:

$$F_{tl}^{ds}(t,\vartheta) = \frac{\sin(\beta)}{\sin(\alpha+\beta)} F_y(t,\vartheta)$$

$$F_{ll}^{ds}(t,\vartheta) = \frac{\sin(\alpha)}{\sin(\alpha+\beta)} F_y(t,\vartheta)$$

Herein the time dependant angles $\alpha = \alpha(t)$ and $\beta = \beta(t)$ were used to describe the limb's deviation from exact vertical orientation (Fig. ESM1). Both were determined using trigonometric relations and accounted for the instantaneous locations of SP, described by $\Delta x_{sp}(t)$ and $y_{sp}(t)$, and horizontal ground contact coordinates $x_{ll}(t)$ and $x_{tl}(t)$ of the leading and trailing limbs. Vertical coordinates $y_{ll}(t)$ and $y_{tl}(t)$ of ground contact were equal to zero at all times due to a coordinate system which was defined relative to the body of the individual (Fig. 4). Thus, the powers of the leading and trailing limb, respectively, were:

$$P_{tl}^{ds}(t,\vartheta) = F_{tl}(t,\vartheta)\sin(\alpha)(v_m + \Delta v_{hsp}) + F_{tl}(t,\vartheta)\cos(\alpha)v_{sp}(t)$$

$$P_{ll}^{ds}(t,\vartheta) = -F_{ll}(t,\vartheta)\sin(\beta)(v_m + \Delta v_{hsp}) + F_{ll}(t,\vartheta)\cos(\beta)v_{sp}(t)$$

Again, positive and negative work of the leading and trailing limb, respectively, were determined through integration of powers over time:

$$W_{tl/ll}^{ds+/ds-}(\vartheta) = \frac{1}{2}\int_{t_B(ds)}^{t_E(ds)}(P_{tl/ll}^{ds}(t,\vartheta) \pm \left|P_{tl/ll}^{ds}(t,\vartheta)\right|)\,dt$$

In a complete stride cycle the SP runs through two phases of single limb support and another two phases of double limb support. As a result, the metabolic energy costs for bearing the load of the head-neck unit with respect to the phase shift between the vertical oscillations of the unit's COM and the individual's thorax finally amounted to:

$$\Delta E_m(\vartheta) = 2\left\{4\left(\sum_{i,k} W_i^{k+}(\vartheta)\right) + \frac{5}{6}\left|\left(\sum_{i,k} W_i^{k-}(\vartheta)\right)\right|\right\}$$

Not included here was the metabolic cost of protruding the non-supporting limb, since its contribution to energy consumption is identical to all patterns of walking discussed here and does not vary with phase shift. Furthermore, limb protrusion is achieved mainly passively as the inertial properties of the respective limb match those of a suspended pendulum operating at Eigen frequency[7].

References

1. Buchner HHF, Savelberg HHCM, Schamhardt HC, Barneveld A. 1997 Inertial properties of Dutch Warmblood horses. *J Biomech* **30**, 653–658.
2. Berry HH, Siegfried WR, Crowe TM. 1982 Activity patterns in a population of free-ranging wildebeest *Connochaetes taurinus* at Etosha National Park. *Zeitschrift fur Tierpsychologie* **59**, 229-246.
3. Boyd L, Carbonaro D, Houpt K. 1988 The 24-hour time budget of Przewalski horses. *Appl Ani Behav* **21**, 5–17.
4. Gellman KS, Bertram JEA, Hermanson JW. 2002 Morphology, Histochemistry, and Function of Epaxial Cervical Musculature in the Horse (*Equus caballus*). *J Morph* **251**, 182–194.
5. Griffin TM, Main RP, Farley CT. 2004 Biomechanics of quadrupedal walking: how do four-legged animals achieve inverted pendulum-like movements? *J Exp Biol* **207**, 3545–3558.
6. Merkens HW, Schamhardt HC, Hartman W, Kersjes AW. 1985 Ground reaction force patterns of Dutch Warmblood horses at normal walk. *Equine Vet J* **18**, 207-214.
7. Witte H, Lesch C, Preuschoft H, Loitsch C. 1995 Die Gangarten der Pferde: Sind Schwingungsmechanismen entscheidend? Teil I: Pendelschwingungen der Beine bestimmen den Schritt. *Pferdeheilkunde* **11**, 199-206

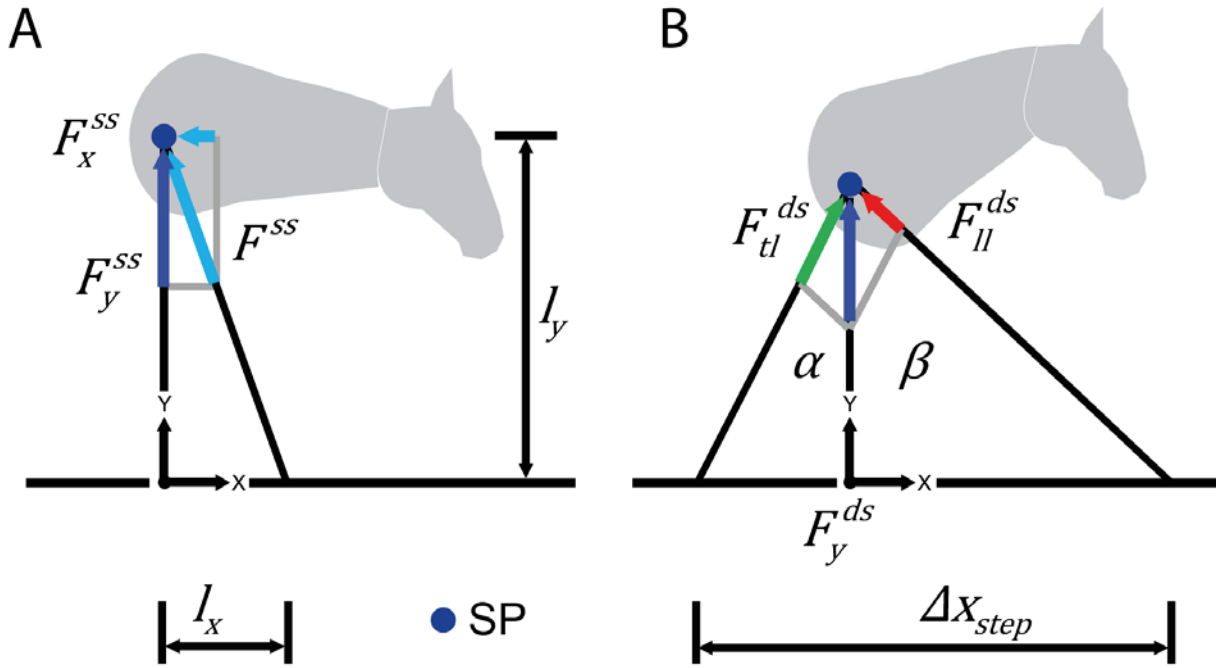

Fig. ESM1: Inverse dynamics approach used for the analysis of vertically directed forces of the supporting limbs at the trunk-forelimb suspension point (SP) necessary to maintain the movement of the simple horse model during single support phase (ss) and double support phase (ds). Symbols are explained in the text.

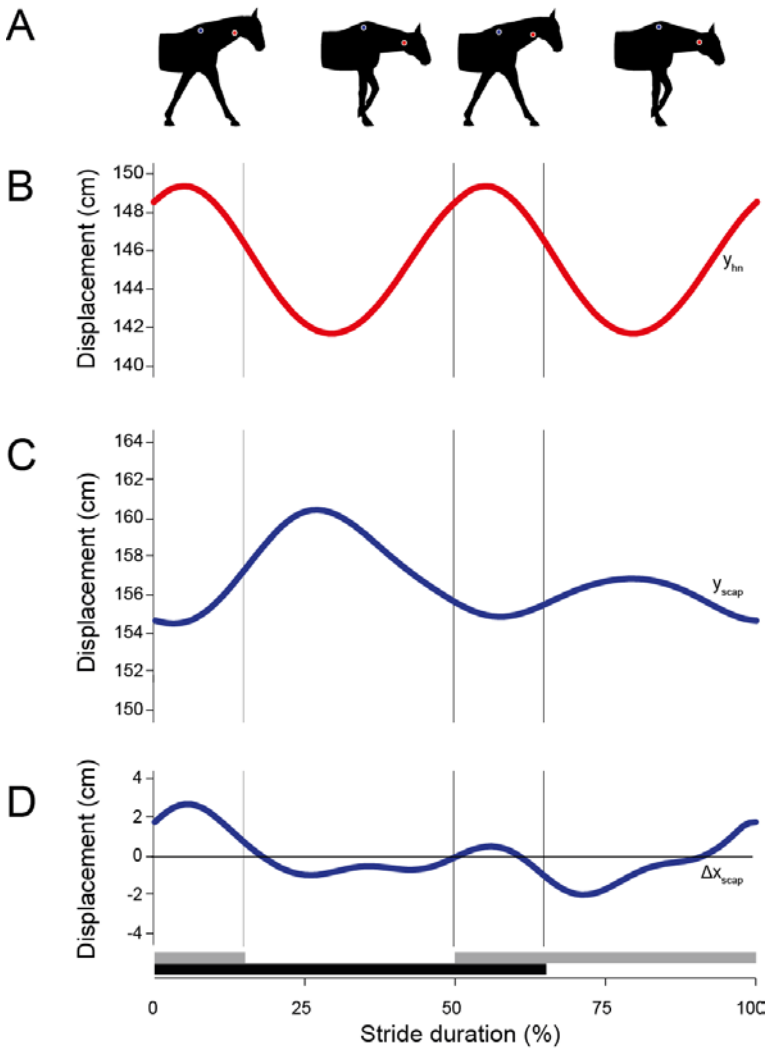

Fig. ESM2: Mean kinematic profiles (N = 5) over an entire stride derived from motion capturing of a reference individual. A: Schematic representation of scapula marker (blue) and the approximated instantaneous position of the head-neck unit COM (red). B: The vertical displacement of the of the head-neck unit's COM (y_{hn}). C: The vertical displacement of the scapula marker (y_{scap}) of the limb that starts the stride at 0% (duration of support phase represented by black bar). D: The horizontal displacement of the scapula marker (Δx_{scap}) used for the model's SP. The vertical lines depict the ends/beginnings of single support and double support phases. Note that horizontal displacements of the head-neck unit's COM were found to be minimal (< 0.3 cm) and not considered in the model. For the analytic model, instantaneous marker positions during the entire support phase of a limb (i.e., two double support phases and 1 single support phase) were approximated using either harmonic or spline functions (see text).